Tomographic presentation of temperature profiles in a convective heat flow by high resolution holographic interferometry

D.Vukićević

Institute of Physics of the University Zagreb,
Bijenicka 45, YU 41000 Zagreb

H.Jäger, T. Neger, H. Philipp, J. Woisetschläger

Institut für Experimentalphysik der Technischen Universität Graz,
Petersgasse 16, A 8010 Graz

ABSTRACT

The aim of these investigations is the development of a new experimental setup, allowing multidirectional analysis of phase objects by high resolution holographic interferometry. With this setup it is possible to obtain interferograms of finite width covering a range of view of 155°. The first tests were performed on a stabilized convective heat flow, since its temperature distribution could be measured with an NTC-detector, providing reference data to check the quality of the tomographic reconstructions.

To obtain highest resolution of the interferometric data, the holographic interferograms were evaluated using the formalism of the fast Fourier transformation (FFT).

The distributions of the index of refraction were obtained by two commonly used tomographic reconstruction procedures: the convolution method and the algebraic reconstruction technique (ART) showing better results, especially if the projection data are not completely covering 180° of view.

1. INTRODUCTION

On the problem of diagnosing inhomogeneous transparent media (e.g. gas flows, plasma jets, switching sparks, welding arcs) many investigations have been carried out until now by using a formalism for data reduction based on the Abel inversion technique assuming rotational symmetry of the phase object. Unfortunately the experimental conditions frequently cannot be satisfactorily adjusted to obtain this symmetry type with the required accuracy. Only a small number of authors have tried to modify the inversion techniques for asymmetric phase objects by different extensions of the Abel inversion procedure. On the other hand the X-ray computer tomography in medicine gives a completely spatial resolution over 360° of strongly inhomogeneous matter by applying suited reconstruction techniques. Our investigation should be understood as an attempt to apply the mathematical formalism of computer tomography to experimentally obtained optical data, especially by multidirectional holographic interferometry.

2. EXPERIMENTAL

2.1 Optical setup

Holographic interferograms of inhomogeneous transparent media (phase objects), which are recorded according to fig. 1, do not provide a multidirectional view of the interferogram from different directions. It is obvious that an arrangement with a diffusing screen[1] (fig. 2) must be chosen as a basic requirement in order to observe phase inhomogeneities by interferometry in a multidirectional way. The inhomogeneous zone - now being penetrated by light scattered from every point of the screen - can be investigated by a single hologram from different directions within a certain angular range.

The optical arrangement is shown in fig. 3. To obtain the largest possible angle of view the double exposure interferograms were recorded as reflection type holograms, allowing the observation of a phase object within 155°. In a specially designed real time plate holder HX three holographic plates are facing three diffusing screens.

In order to evaluate the phase shift of the interferograms using a Fourier transfomation algorithm, a vertical reference fringe system had to be superposed. This was achieved by rotating one common mirror RM. With a sandwich hologram SH[2], that allows to compensate the reference fringes by tilting it, the stability of the phase object during the exposure can be checked.

After developement the holograms were repositioned and the interferograms could be

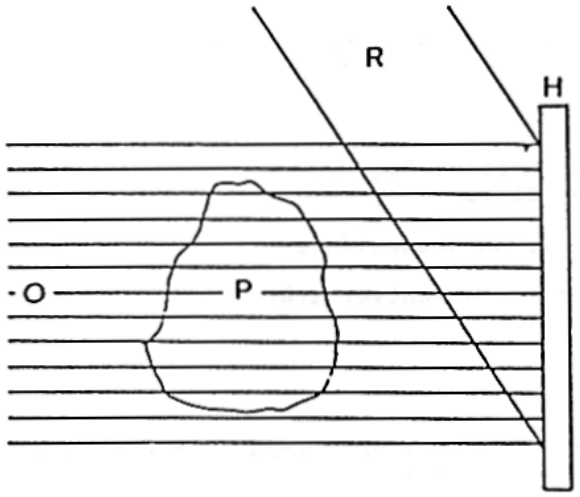

Figure 1. Recording a holographic interferogram without a diffusing screen (H holographic plate, O object beam, R reference beam, P phase inhomogeneity).

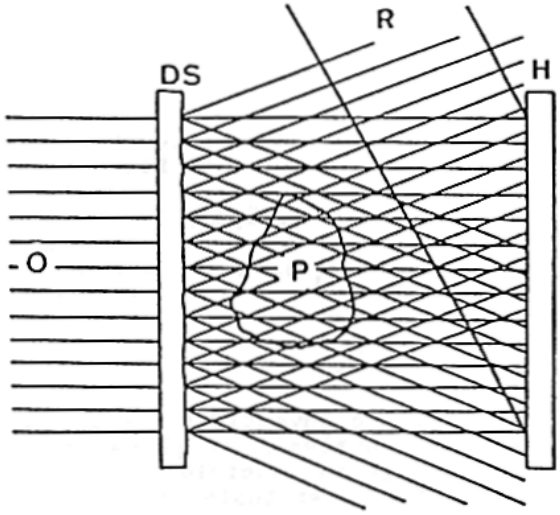

Figure 2. The use of a diffusing screen DS, providing multidirectional observation of the interferograms of inhomogeneous transparent phase media.

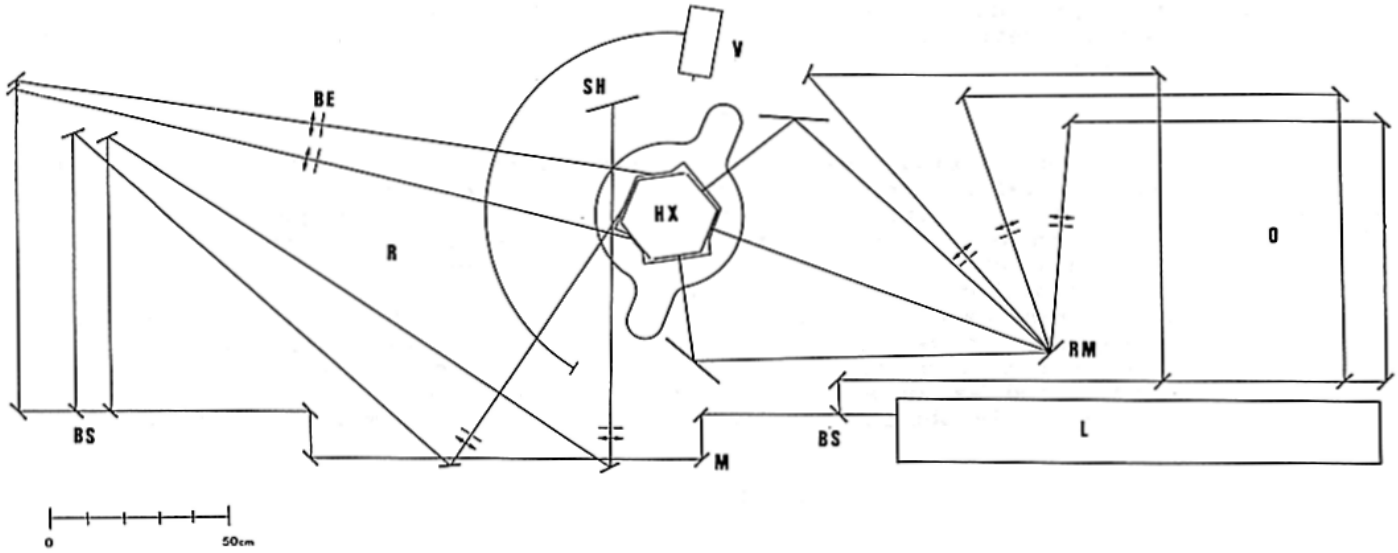

Figure 3. The complete optical arrangement for simultaneous recording of multidirectional holographic interferograms (O object beams, R reference beams, RS reference beam for sandwich hologram SH, RM mirror for simultaneous rotation of the three object beams, HX hexagonal plate holder, BS beamsplitters, BE beamexpanders).

recorded using a video camera and a video frame store (786*256 pixels, 6 bit intensity resolution). The video camera could be scanned along an arc of 180° at the reference beam side.

2.2 Realisation of phase inhomogeneities for testing purposes

A cross-section of the device producing the inhomogeneous phase object is shown in fig. 4. The central cone and the surrounding part - both made from aluminium, being electrically heated at the bottom - establish a cavity, through which air flows and increases its temperature. The inlets for the air supply are equidistant radially drill holes through the outer aluminium cylinder to ensure an uniform flow. By a heat insulation, a cover of a water-cooled aluminium sheet and an electronic stabilisation of the heating current stationary conditions between the heated part, the cooled part and the surrounding air could be achieved in that way, that the surface temperature at the top of this cover sufficiently equals that of the surrounding medium. In this way an additional change of the refractive index around the real test zone is suppressed. The geometry of the phase

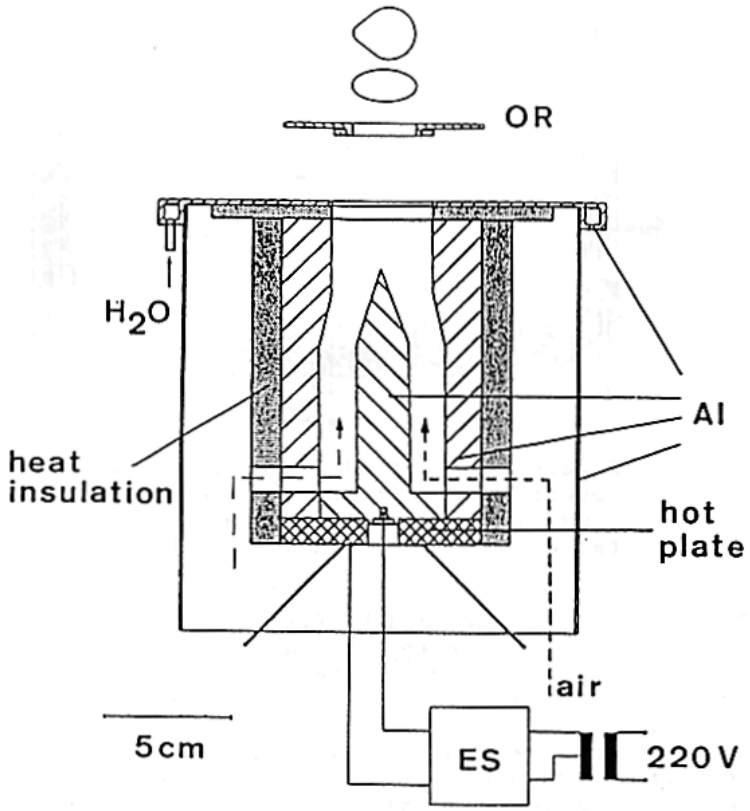

Figure 4. The device for the production of a stationary heat flow (ES electronically stabilized source for heating current, OR orifice for determining the flow geometry)

inhomogeneity caused by the emerging air flow can be influenced by choosing orifices of different shapes (compare top of fig. 4).

An independent measurement of the temperature distribution in the hot flow is possible with an NTC (negative temperature coefficient) detector. Its size is smaller than 0.5 mm, thus giving nearly dot-like resolution. Using a pantograph (3:1) this sensor can be scanned in horizontal planes at different heights. After heating for half an hour the convective heat source reaches stable conditions and does not vary more than 0.5°C at the maximum temperature value afterwards. By real time holographic interferometry it was proved that the sensor has negligible influence on the temperature distribution and does not affect the flow conditions.

3. EVALUATION OF ANGULAR DEPENDENT PHASE SHIFTS

Fig. 5 shows a typical intensity plot of an interferogram for a certain height z above the orifice (z = 13.5 mm). For further data reduction a range of 512 pixels was chosen from the total stored 786. The application[3] of the fast Fourier transformation to the intensity distribution i(p)

$$i(p) = i_o(p) + h(p)\cdot\cos(2\pi\nu_o p + \Phi(p)) \equiv i_o(p) + g(p) + g^*(p)$$

$$\text{with} \quad g(p) = 1/2\, h(p)\cdot\exp(i(2\pi\nu_o p + \Phi(p))) \qquad (1)$$

$$g^*(p) = 1/2\, h(p)\exp(-i(2\pi\nu_o p + \Phi(p)))$$

$$\Phi'(p) = 2\pi\nu_o p + \Phi(p)$$

(p horizontal coordinate, h the modulation depth of the fringes, Φ phase change by the inhomogeneous medium, ν_o superimposed carrier frequency for optical heterodyning, the first term i_o describes the mean intensity) leads to frequency dependent presentation of the intensity

$$I(\nu) = I_o(\nu) + G(\nu) + G^*(\nu) \qquad (2)$$

(see for example fig. 6, the capital letters being used for the Fourier transforms).

The problem now arises to separate the relevant information on the phase change caused by the investigated inhomogeneous phase object from the frequency spectrum. A multiplication of

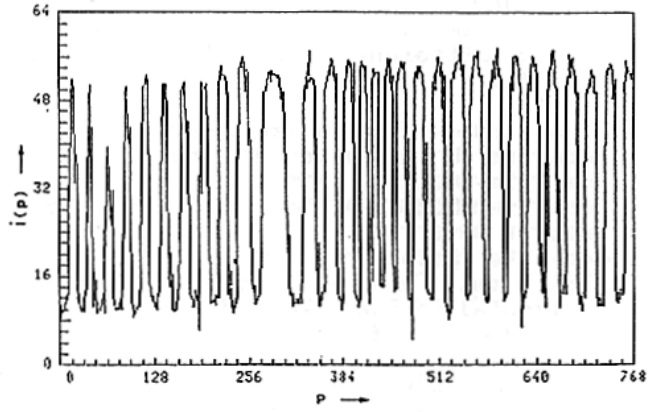

Figure 5. Fringe pattern intensity distribution i(p) of an optically heterodyned phase object interferogram along a horizontal column. The unit pixel distance p is 0.0875 mm.

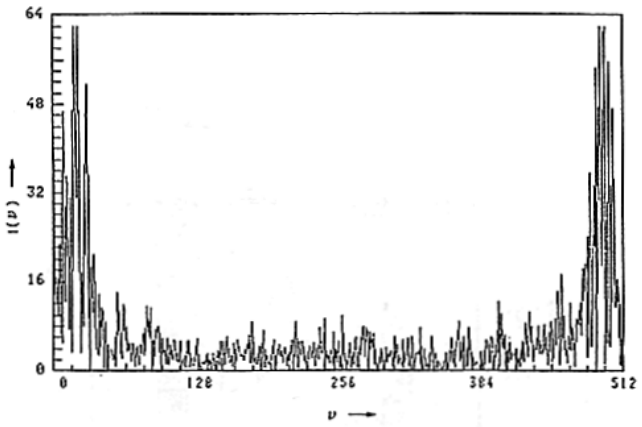

Figure 6. Spatial frequency amplitude spectrum I(ν) of the fringe pattern intensity distribution from fig. 1, obtained by fast Fourier transformation.

this spectrum I(ν) by a window function of suitable bandwidth f(ν) yields G(ν) and suppresses $I_o(\nu)$, the frequency spectrum of the mean intensity of the interferogram. An inverse Fourier transformation of G(ν) gives g(p) (compare equs.1), taking the arcustangens of imaginary and real part of g(p) the relative phase distribution $\Phi'(p)$ is obtained (see fig. 7), which is still dominated by the carrier frequency. A linear regression in the "undisturbed" parts with respect to the modulation by the phase change $\Phi(p)$ stemming from the phase object enables a substraction of the phase change caused by the carrier frequency ν_o, leading to the interesting phase distribution $\Phi(p)$ (fig. 8). In connection with the tomographic reconstruction methods these distributions - which are characteristic for different observation angles - are also referred as "projection data".

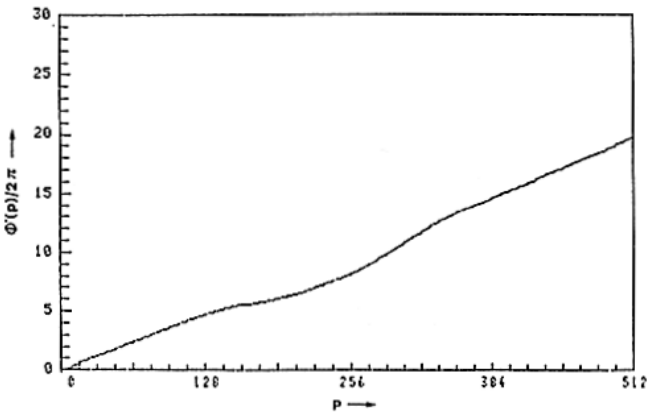

Figure 7. Relative phase change distribution $\Phi'(p)$ derived from an optical heterodyned interferogram.

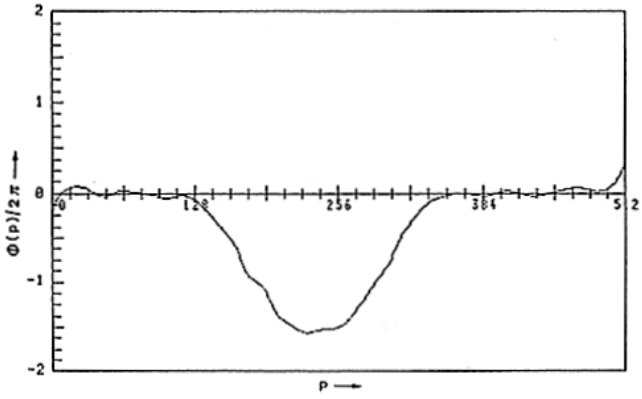

Figure 8. Sub fringe analysed phase shift $\Phi(p)$ caused by the hot air flow.

4. TOMOGRAPHIC CALCULATION OF THE LOCAL INDEX OF REFRACTION

4.1 Convolution method

The sets of projection data given as phase distributions

$$\Phi(p,\Theta) = 2\pi/\lambda \int_{-\infty}^{+\infty} ((n(r,\varphi) - n_o))\, ds \qquad (3)$$

(the meaning of the symbols is shown in fig. 9) could now be subject to an inverse Radon transform,

$$\frac{2\pi}{\lambda}(n(r,\varphi)-n_o) = \frac{1}{2\pi^2}\int_0^{\pi} d\Theta \int_{-\infty}^{+\infty} dp \; \frac{1}{r\cos(\Theta-\varphi)-p} \cdot \frac{d\Phi(p,\Theta)}{dp} \quad . \tag{4}$$

This procedure can be described by a differentiation, a subsequent Hilbert transformation and finally a backprojection. The essential advantage of the socalled convolution method[4] is based on the mathematically exact substitution of the differentiation and the Hilbert transformation in equ. 4 by convolution with an appropriate function,

$$\frac{2\pi}{\lambda}(n(r,\varphi)-n_o) = \int_0^{\pi} d\Theta \int_{-\infty}^{+\infty} dp \; \Phi(p,\Theta) \cdot \rho(r\cos(\Theta-\varphi)-p) \tag{5}$$

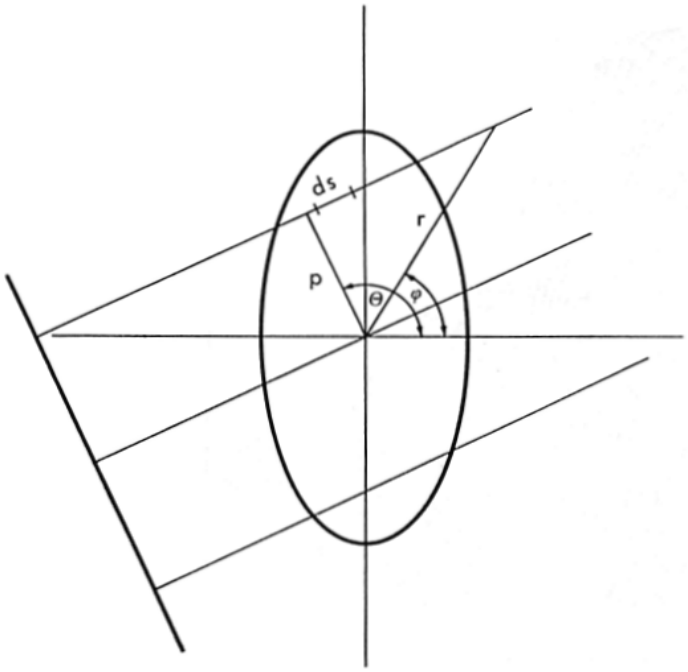

Figure 9. Projection data collection for tomography: Explanation of symbols.

the choice of which has mainly influence on the resolution and the smoothing of the reconstructed refractive index distribution.

If the set of interferograms is not complete - that means not equally spaced within a range of view of 180° - the missing phase distributions have to be compensated. A possibility is to incorporate symmetry assumptions (fig. 10). Linear interpolation[5] of the missing phase distributions (fig. 11) avoids symmetry assumptions and is easily performed with a computer.

4.2 Algebraic reconstruction technique

In contrast to the convolution method, that solves the Radoninversion analytically, the ART-algorithms are selfconsistent iterative approaches.

The simplest ART-algorithm starts from a first approximation of the field of the index of refraction (e.g. obtained by the convolution method). The line integrals of the Radontransformation (equ. 5) are calculated from the approximated field. The field of the index of refraction is corrected along the path of the interferograms by the difference of the measured phase and the calculated phase divided by the length of the beam in the testzone. This procedure is repeated until the resulting field converges toward a stable solution.

Here a more sophisticated approach was used[4]:
- the measurement error of the phase distributions is taken into account;
- since the index of refraction of the hot air in the convective heat flow is less than the one of the undisturbed air, $(n(r,\varphi)-n_o)$ is set zero, if it gets greater zero by a correction;
- to suppres noise in the reconstruction, the field of the index of refraction is "selectivly" smoothed after one complete iteration by assigning each pixel the weighted mean of its nearest neighbours.

ART is very attractive, since missing projections may simply be neglected[5] and the reconstruction is less noisy (especially in regions far from the center). Fig. 12 shows a result obtained by ART.

5. RESULTS AND DISCUSSION

Fig. 10, 11 and 12 show spatially resolved temperature distributions obtained for a horizontal plane in z = 13.5 mm height above the orifice of the hot air flow source, having an elliptical shape (fig. 10), respectivly an egglike shape (fig. 11, 12). The temperature values were derived by using tables[6] for the dependence on the refractive index.

In the case of elliptical geometry the temperature field was calculated from 19 interferograms equally spaced by the convolution method under the assumption of symmetry to the short semiaxes of the elliptical orifice of the heating device (fig. 4). The temperature distribution in the heat flow was measured at 17*17 points. The maximum deviation from the directly measured values was 6.2°C, the mean absolute deviation 2.5°C adequate to 5% of the mean temperature value.

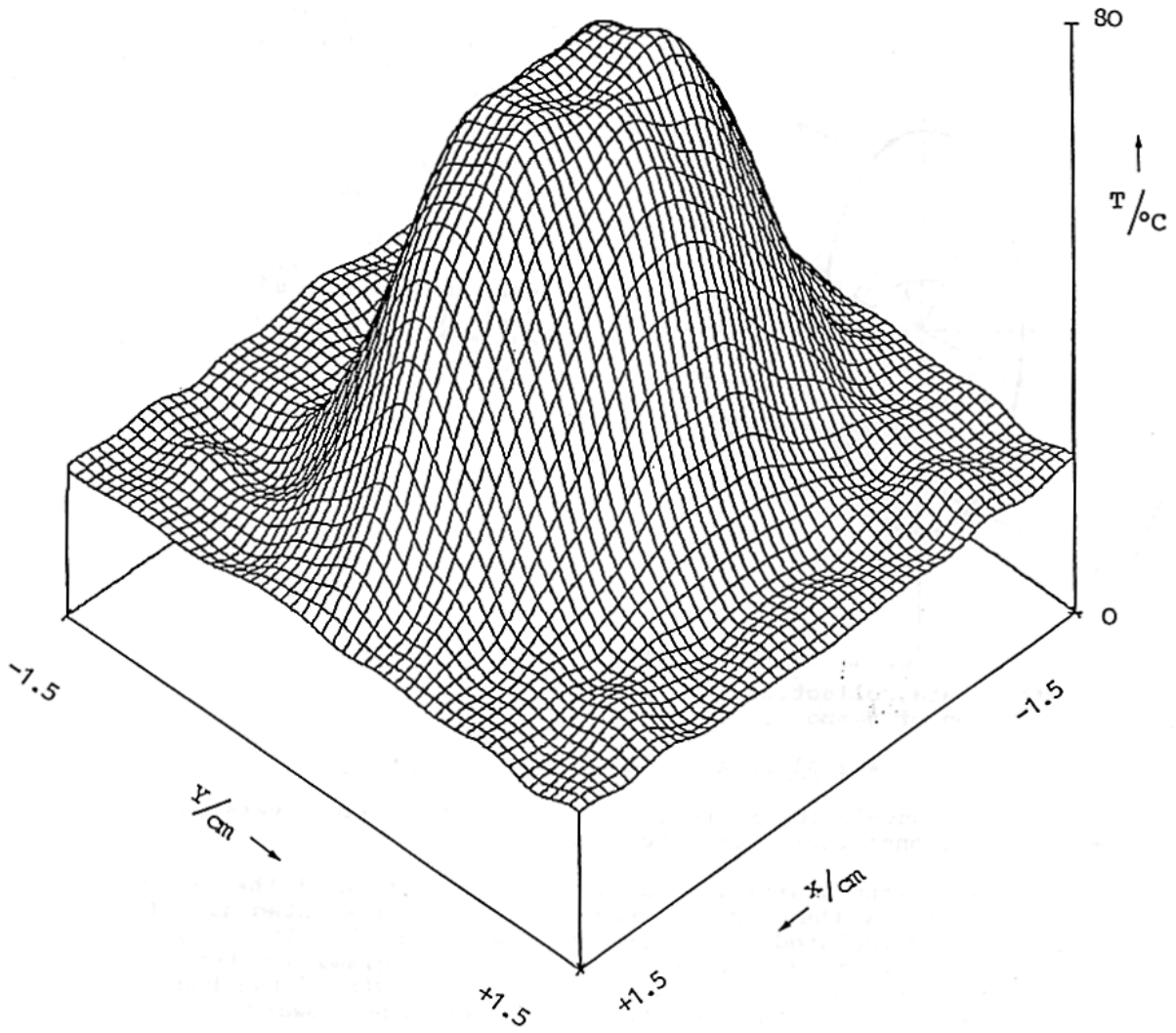

Figure 10. Temperature distribution of a convective heat flow of elliptical geometry (convolution method)

The temperature field in the heat flow with eggshaped geometry was obtained from 27 interferograms, mostly spaced by 5°, by the convolution method with linear interpolation of the missing phase distributions (fig. 11). The maximum deviation was 12°C, the mean absolute deviation 3.5°C adequate to 9% of the mean temperature value.

Starting from the field of the index of refraction obtained by the convolution method, the ART algorithm was used to improve the result (fig. 12). After 5 complete iterations the changes of the resulting fields were negligible. The maximum deviation was 10.2°C, the mean absolute deviation 2.8°C adequate to 7% of the mean temperature value.

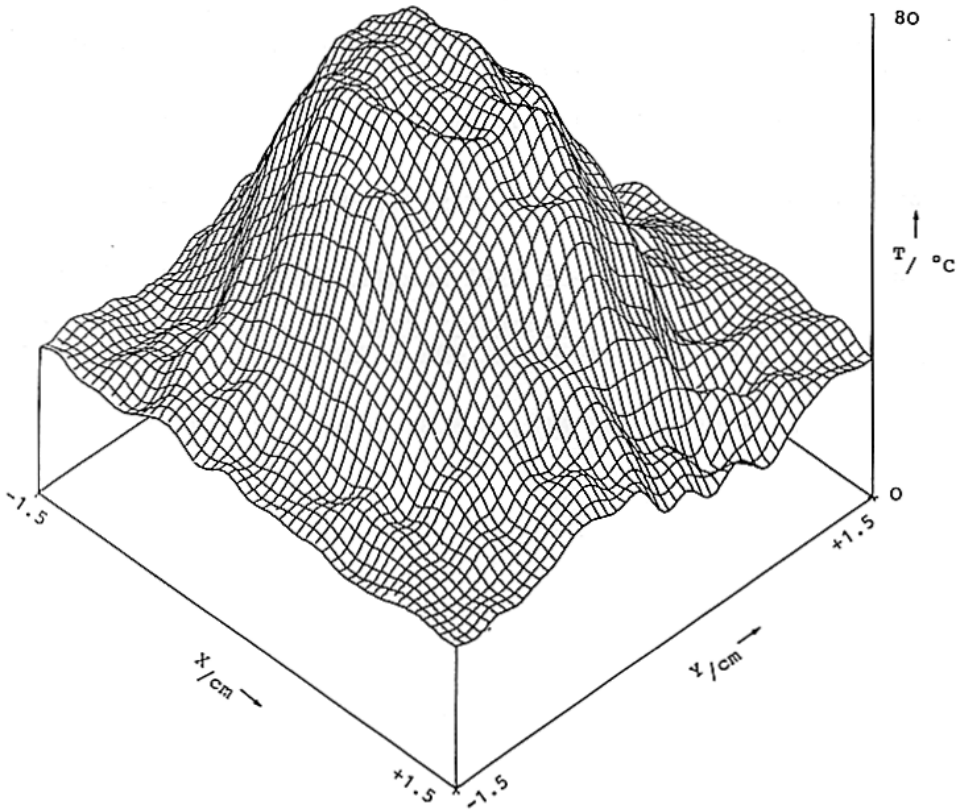

Figure 11. Temperature profile of a convective heat flow of eggshaped geometry (convolution method).

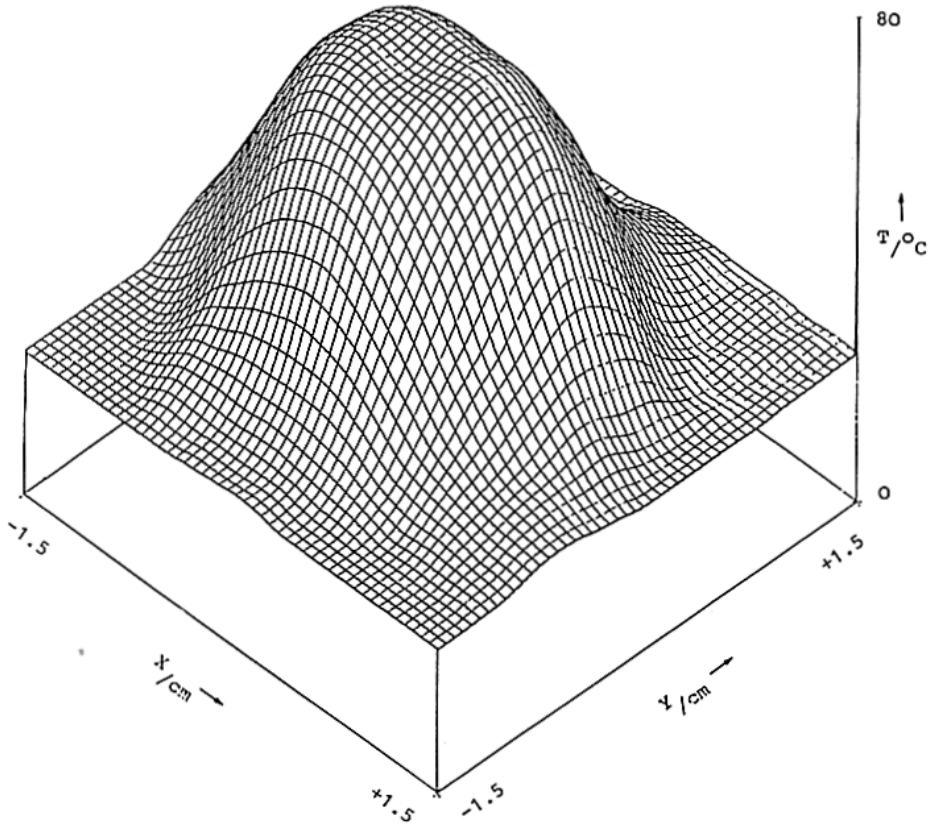

Figure 12. Temperature profile of a convective heat flow of eggshaped geometry (ART).

REFERENCES

1 Y. I. Ostrovsky, M. M. Butusov and G. V. Ostrovskaya, Interferometry by Holography, Springer Verlag Berlin - Heidelberg - New York (1980)

2 N. Abramson, The Making and Evaluation of Holograms, Academic Press (1981)

3 A. Džubur and D. Vukičević, Ultrahigh resolution sandwich holography, Appl. Opt. 23, 1474 (1984)

4 G. T. Herman, Image Reconstructions from Projections, Academic Press (1980)

5 B. E. Oppenheim, Reconstruction Tomography from Incomplete Projections, in Reconstruction Tomography in Diagnostic Radiology and Nuclear Medicine, University Park Press (1977)

6 E. F. Jones, The Refractivity of Air, N.B.S. Journ. of Res. 86, 27 (1981)